Study of Joint Effect on Pipe in Pipe Jacking Method

L. G. Le[1], M. Takise[1], M. Sugimoto[1] and K. Nakamura[2]
[1]*Civil Engineering Department, Nagaoka University of Technology, Nagaoka, Japan*
[2]*Technology Development Division, Fujimura Hume Pipe Co., Ltd., Kashiwazaki, Japan*
E-mail: sugimo@vos.nagaokaut.ac.jp

ABSTRACT: Recently, pipe jacking method has become popular in micro tunnelling because of its benefits for economy and environment. However, jacked pipes have complex performance during installation process, particularly when the pipes are driven through a curved alignment. In such a case, the joints between the pipes significantly affect the behaviour of the pipes and the alignment deviation. To investigate the influence of joints on pipes, full scale tests and numerical modelling were carried out to simulate pipe jacking of two consecutive pipes in both straight and curved alignments. It was found that stress concentration occurs along pipe length at the range where cushion materials are set for both alignments and at the concave side of curve for the curved alignment. In addition, it was confirmed that the stack pipe model gives a reasonable result to simulate the experiments for the pipe jacking method.

1. INTRODUCTION

Pipe jacking method has been widely used for installing underground pipelines for various issues such as electricity, water, gas, and railway etc. because of its benefits for economy, environment, and construction safety over open cut method, particularly in congested areas. Due to the demand of society development, the requirement of pipe jacking involved in big projects becomes more difficult due to large jack force applied and complex ground condition. They are challenging for engineers as well as researchers because it is not easy to get an exact solution due to the influence of many factors during installation process. Many parameters at each construction stage, e.g. penetration rate, over-cutting size, lubrication material, stoppage duration, alteration of ground condition and overburden pressure, must be considered to achieve a good result (Pellet-Beaucour and Kastner, 2002; French Society for Trenchless Technology 2006).

Norris (1992) demonstrated that small angular deviations between successive pipes caused severe localized stresses on the pipe ends. In fact, joints between pipes are the most important factor which influences stress distribution on pipes, especially when pipes are driven in curve conditions. Study on the influence of joints is, therefore, needed. Dietmar et al. (2007) presented a new statics method of computing and controlling pipe jacking that can take load-distribution effects into account to observe and prevent excess jacking load during installation process. Bert and Bernhard (2008) investigated the effects of alignment and different kinds of transmission rings. Peter et al. (2009) suggested a hydraulic joint which provides more uniform stress profile at the pipe ends compared to the traditional joint. To reduce the stress concentration on pipes driven under curved conditions, Le et al. (2012) introduced a joint design with cushion equipped at the top and bottom of pipes.

To better understand the behaviour of pipe jacking and the effect of joints on pipes and to reduce damage potential and improve design for pipe jacking, full scale tests for two consecutive pipes were carried out for both straight and curved alignment cases. Furthermore, numerical simulation of the experiments was performed. This paper presents the results from the full scale tests and the numerical analyses and examines the influence of joint on pipes. In addition, the numerical model is also validated.

2. EXPERIMENT

2.1 Testing system

To investigate the pipe jacking manner and the impact of joint to pipes, a full scale testing system was built in the pit with dimension of 13m x 4 m, which can carry out experiments two consecutive on concrete pipes jacking as shown in Figures 1 and 2. The system is composed of two consecutive concrete pipes, a steel ring to transfer jack force to the pipes, two abutments at the both ends connected with steel bars, a jacking frame station involving two hydraulic axial jacks to generate thrust force, eight side jacks including their stations to adjust the alignment and create surrounding pressure, four concrete shell supports at the both sides of the pipes to transpose side pressure to the pipe periphery, and rubber sheets and Teflon sheets inserted between the concrete shell supports and the pipe periphery to ensure stress distribution. Furthermore, grease was spread on the Teflon sheets to reduce periphery friction. The joint between the two pipes was designed including expanded polystyrene (EPS) plate of 40mm in thickness (EPS (40mm)) set in a range of 90 degrees at the top and bottom as shown in Figure 3 and 4. The EPS of 10mm thick (EPS (10mm)) was used at the joint between the steel ring and Pipe II, and between Pipe I and the abutment; it also placed in a range of 90 degrees at the top and bottom. Hydraulic jacks in axial direction were positioned at the top and bottom to create thrust force. Surrounding pressure was generated from eight side jacks located at the left and right sides. Hemispherical pads were mounted at the stressing heads of the hydraulic jacks to cut rotational constraint.

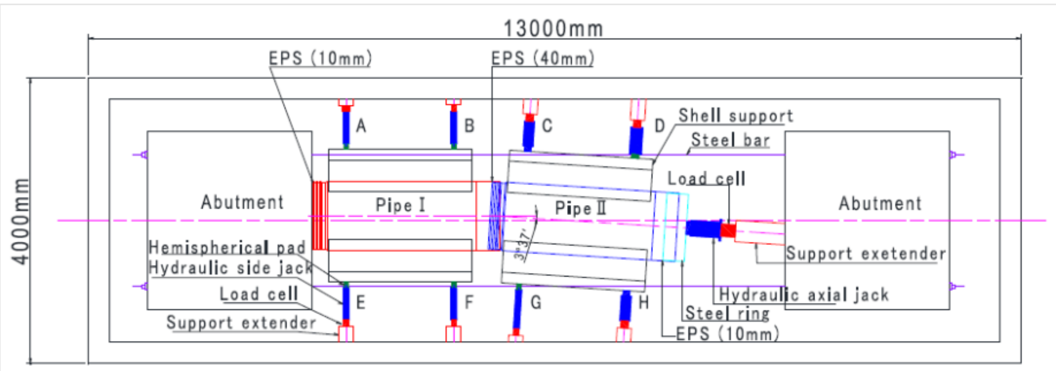

Figure 1 Schematic view of the testing system

Figure 2 Full-scale testing system

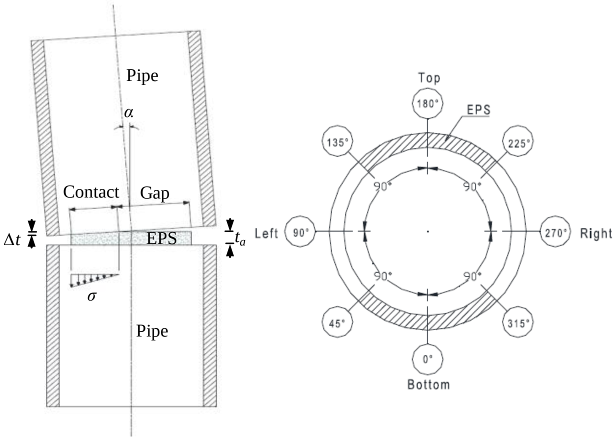

(a) Joint-pipes interaction (b) Cross section view

Figure 3 Joint model

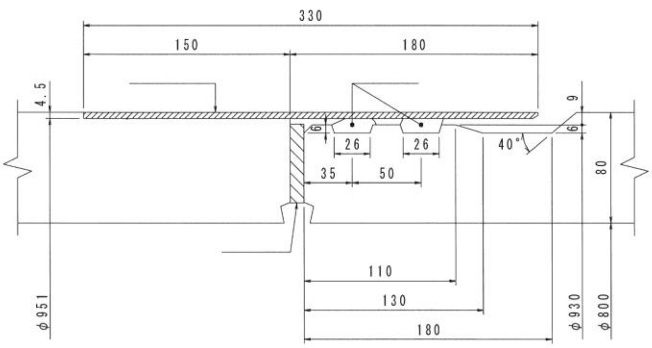

Unit: mm

Figure 4 Joint configuration

2.2 Instrumentation and measurement

Strains in the pipes were measured by strain gauges which were installed at 38 points at the inner side and 26 points at the outer side, as shown in Figure 5, for each pipe. The strain gauges were allocated densely towards the joint between two concrete pipes. The strain gauges were placed in axial, circumferential, and diagonal directions corresponding to 0, 90, and 45 degrees to the axial direction. However, the strain gauges in 45 degrees only focused on the high strain potential area supposed near the joint. Load cells were installed between the jack stations and the bases of the hydraulic jacks to measure jack forces. A load cell was involved for each jack. Furthermore, displacement transducers were placed inside the pipes to measure the deformation of the pipes, at the joint to measure the gap between the pipes, and along the concrete shell supports to determine the movement of the pipes in transverse and axial directions.

All measurement instruments were connected to the data acquisition system. Data were monitored and stored through a computer placed in the control house. During the tests, the following parameters were measured: strain in the pipes, deformation of the pipes, gap between two pipes at the joint, displacement of the concrete shell supports, jacking force, and support force of the pipes in transverse direction.

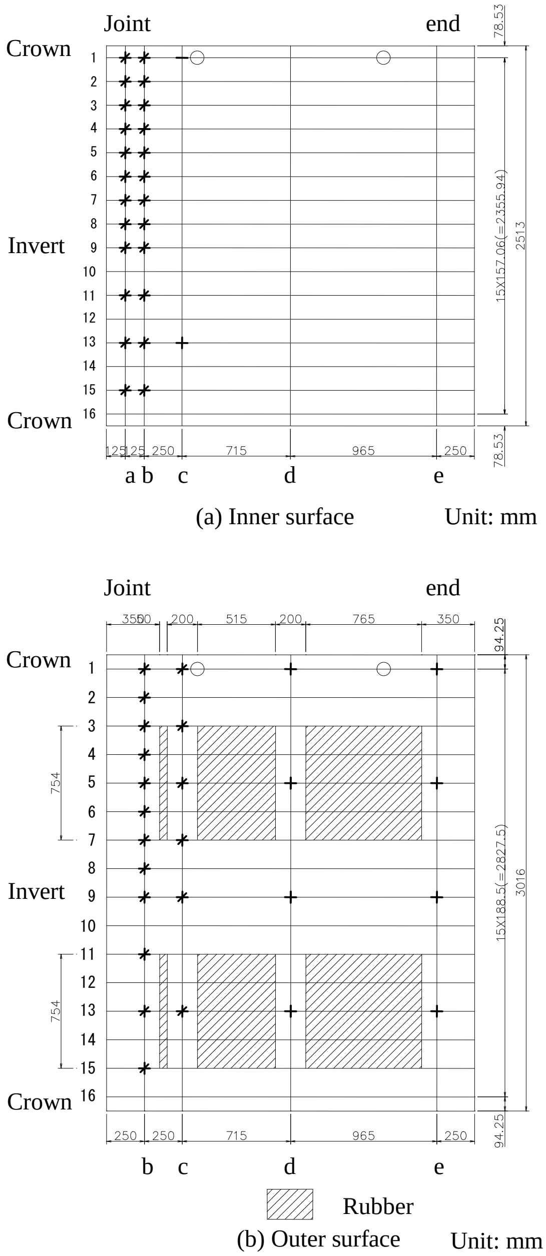

Figure 5 Positions of strain gauges

2.3 Testing program

To investigate the influence of joint to pipes, the tests were done for the cases of straight and curved alignments. The pipes were first installed with strain gauges in advance, then laid on the base of the test system. Other required equipment such as the concrete shell supports, rubber sheets, Teflon sheets, hydraulic jacks, load cells, transducer measurements was erected. Finally, the instruments were connected to data loggers and a computer for execution. The alignment was adjusted through the side jacks and a total station surveying equipment. Initial side force of 20kN for each side jack was applied to generate initial surrounding pressure and maintain the alignment.

For the straight alignment (Case S), thrust force was applied up to 2700kN with interval of 100kN and unloaded with 500kN interval. In case of curved alignment (Case C), a crease angle of 3.61 degrees was designed for the test. The thrust force was conducted up to 1000kN with interval of 50kN and unloaded with interval of 250kN. During the test, data were recorded three times for each jack force step. However, this paper presents and discusses only the case of 1000kN jack force for both straight and curved alignments.

3. NUMERICAL MODELING

To examine the behaviour of the joint and the jacked pipe, numerical modelling of the experiments was constructed. The ground reaction curve proposed by Sramoon and Sugimoto(1999) was used to model the surrounding pressure generated from the side jacks. The EPS joint is represented by joint springs in axial, tangential and radial directions. Stack pipe model introduced by Sugimoto and Asanprakit (2010) was applied to model the execution of the pipe jacking process. Afterwards, simulation was carried out using the experimental data. Subsequently, examination and discussion of the FEM and experiment results are provided. Thus, the model was validated.

3.1 Side reaction model

Ground behaviour surrounding the pipe is very complicated during jacking process. It not only depends on the soil properties but also pertains to many other factors such as pipe shape, excavation method, overcutting, grouting method. But the change of the earth pressure on pipe is basically related to the displacement of the surrounding ground. When ground deforms inwards the pipe periphery, the active state of earth pressure is generated. In contrast, when pipe pushes forwards to the ground, the passive state of earth pressure is produced as shown in Figure 6. Earth pressure acting on the pipe periphery is considered the same way as that on the shield periphery in the kinematic shield model proposed by Sugimoto and Sramoon (2002). To represent the interaction between the ground and the pipe, ground reaction curves in Figure 7 was used, which is expressed as follows

For $U_n \le 0$

$$K_h(U_n) = \left(K_{h0} - K_{h\min}\right)\tanh\left(\frac{a_h U_n}{K_{h0} - K_{h\min}}\right) + K_{h0} \qquad (1)$$

$$K_v(U_n) = \left(K_{v0} - K_{v\min}\right)\tanh\left(\frac{a_v U_n}{K_{v0} - K_{v\min}}\right) + K_{v0} \qquad (2)$$

For $U_n \ge 0$

$$K_h(U_n) = \left(K_{h0} - K_{h\max}\right)\tanh\left(\frac{a_h U_n}{K_{h0} - K_{h\max}}\right) + K_{h0} \qquad (3)$$

$$K_v(U_n) = \left(K_{v0} - K_{v\max}\right)\tanh\left(\frac{a_v U_n}{K_{v0} - K_{v\max}}\right) + K_{v0} \qquad (4)$$

where K_h and K_v are the coefficients of earth pressure in the horizontal and vertical directions, respectively; U_n is the distance from the initial tunnel surface to the pipe (+: outward of tunnel); K_{h0} is the coefficient of earth pressure at rest; K_{v0} is the initial coefficient of vertical earth pressure and normally equals 1; subscripts max and min indicate the upper and lower limits of the coefficients of earth pressure respectively; and a_h and a_v are the slopes of function K_h and K_v at U_n = 0, respectively. Moreover, the coefficient of earth pressure in any direction, K_θ, can be interpolated as

$$K_\theta(U_n,\theta) = K_v(U_n)\cos^2\theta + K_h(U_n)\sin^2\theta \qquad (5)$$

where θ is the angle measured clockwise from the invert as shown in Figure 3b. Finally, the earth pressure normal to pipe surface, σ_n, can be estimated from

$$\sigma_n = K_\theta\,(U_n,\theta)\;\;\sigma_{v0} \qquad (6)$$

To incorporate the characteristics of the rubber sheets into the ground reaction curve, the characteristics of the ground spring for normal surrounding pressure (σ_n) acting on the pipe periphery is obtained as illustrated in Figure 8. The normal stress σ_n is a function of the initial surrounding pressure due to side jacks σ_{n0}, and the pressure change $\Delta\sigma_n$ which depends on the deformation of the rubber sheet U_n. The pre-stress is introduced to represent the initial surrounding pressure, and $\Delta\sigma_n$ is generated during analysis resulting from the deformation of the spring. It is noted that the ground springs are just available at the zones involving the concrete shell supports. The rubber sheets perform linearly with an average Young's modulus of E_{rb} =3933kN/mm^2 until a compression of 5mm. Beyond the compression of 5mm, the rubber sheet is considered very stiff. The ground spring constant, k_{gs} , can be calculated as follows

$$k_{gs} = \frac{E_{eq,rb}A_{gs}}{t_{rb}n_{gs}} \qquad (7)$$

where $E_{eq,rb}$ is the equivalent Young's modulus of the rubber sheet, which is obtained taking account of the actual area covered by the rubber sheets and the area setting the ground springs (=0.61 E_{rb}); A_{gs} is the area setting the ground springs; t_{rb} is the thickness of the rubber sheet; n_{gs} is number of the ground springs.

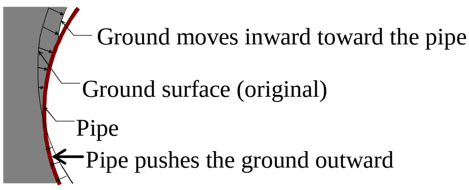

Figure 6 Definition of ground displacement

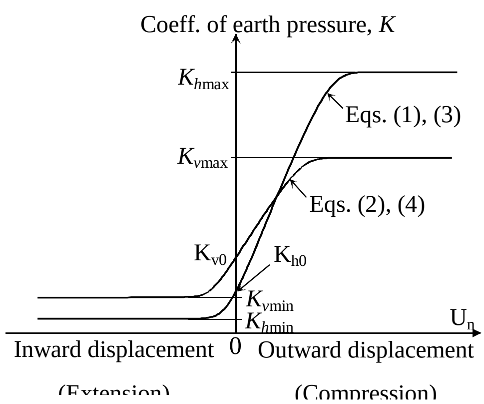

Figure 7 Ground reaction curve

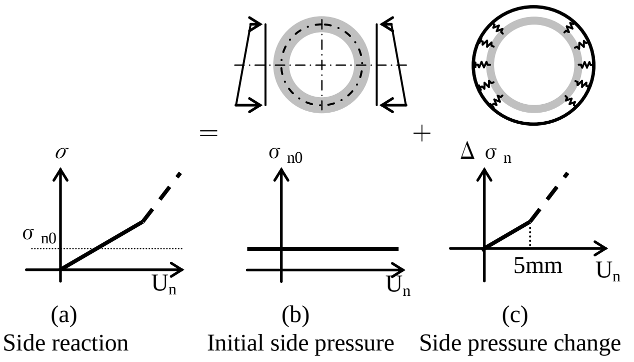

Figure 8 Interaction between side pressure and pipe periphery

3.2 Joint model

Stress distribution due to the joint is correlated with the crease angle, joint cushion characteristics, and geometry of the cushion. Figure 3 shows the EPS joint design and its behaviour due to bending a crease angle α . The largest deformation Δt of the EPS of initial thickness t_a occurs at the edges of the EPS. Thus, the stress σ on the pipe is largest at the edge the EPS. While for the straight alignment, deformation of the EPS and the stress distribution are more uniform.

In this study, joint springs were employed to model the compression effect of the EPS in axial direction and the shear effect in radial and tangential direction. The joint spring model is illustrated in Figure 9. The characteristics of the joint springs are determined as follows:

Joint spring in axial direction: The stress-strain relationship of the EPS(40mm) is shown in Figure 10, where the relationship from 0% to 50% strain was derived from the manufacturer' catalogue (Sekisui Plastic Co., Ltd. 2004), and the gradient of the curve with over 50% strain was assumed to be 100 MN/mm for the whole cushion. Base on Figure 10, taking into account the thickness of the cushion and the number of joint springs, the characteristics of the joint spring in axial direction were set as shown in Figure 11(a) and Table 1.

Joint spring in radial and circumferential direction: The shear behaviour between two pipes is defined by the shear deformation of the cushion, the compressive deformation of the watertight rubber ring at the joint, and the deformation of the pipe collar (as shown in Figure 4). The spring constant of the joint spring in the radial and circumferential direction ks can be expressed by

$$k_s = \frac{L_c hE}{2t_a(1+\nu)} \tag{8}$$

where L_c = length of cushion for one joint spring; h = width of cushion; E = Young's modulus of the cushion material; t_a = thickness of cushion; and ν = Poisson's ratio, since the shear stiffness due to the cushion is two orders in magnitude higher than that due to the watertight rubber ring. Furthermore, since the watertight rubber ring loses elastic characteristics with over 50% strain, which is equivalent to 2.75 mm relative displacement in the radial direction, the pipe can be regarded to touch the pipe collar at the 2.75 mm relative displacement. The spring constant is then defined so that 100 MN/mm at one joint is generated over the 2.75 mm relative displacement. The characteristics of the joint spring in the radial and circumferential direction are then set as shown in Figure 11(b) and Table 1.

3.3 Pipe jacking model

Stack pipe model proposed by Sugiomto and Asanprakit (2010) was employed to carry out the analysis of the experiments. The model specifies pipes into four types depending on their position in the alignment, as shown in Table 2, where PF and PR are the connection points at the front and rear end of each pipe. The phase analysis is applied to analyse throughout the complete alignment as demonstrated in Figure 12. In which, R_P is the outer radius of the pipe; R_T = R_P + initial length of the ground spring; r_{BC} is the coordinates of the point at beginning curve; r_{p1} and r_{p2} are the coordinates of the pipe position before and after applied enforced displacement, respectively; r_{g1} and r_{g2} are the coordinates of the outer end of the ground spring before and after applied enforced displacement, respectively.

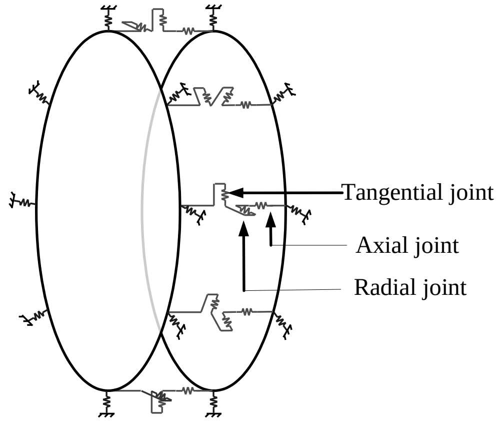

Figure 9 Joint spring model

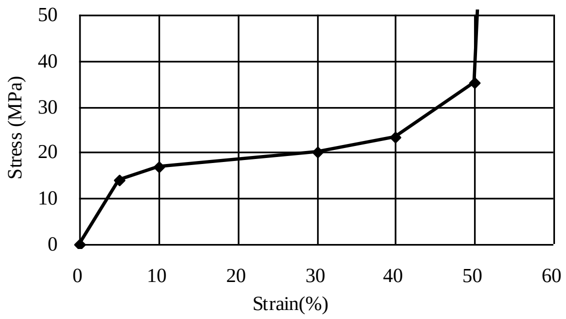

Figure 10 Stress-strain relationship of EPS(40mm)

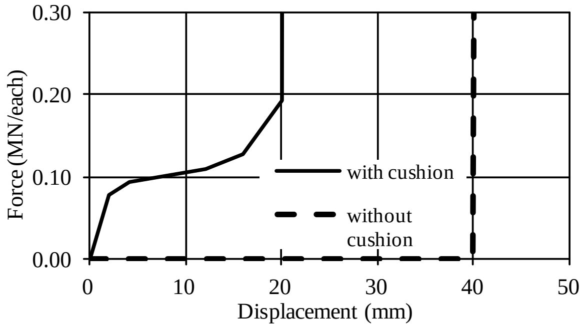

(a) Axial direciton

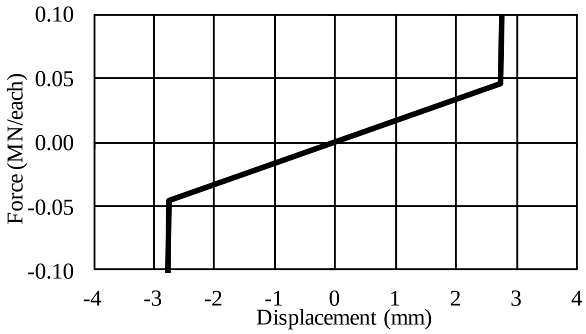

(b) Radial and circumferential direction

Figure 11 Characteristics of joint spring with EPS(40mm)

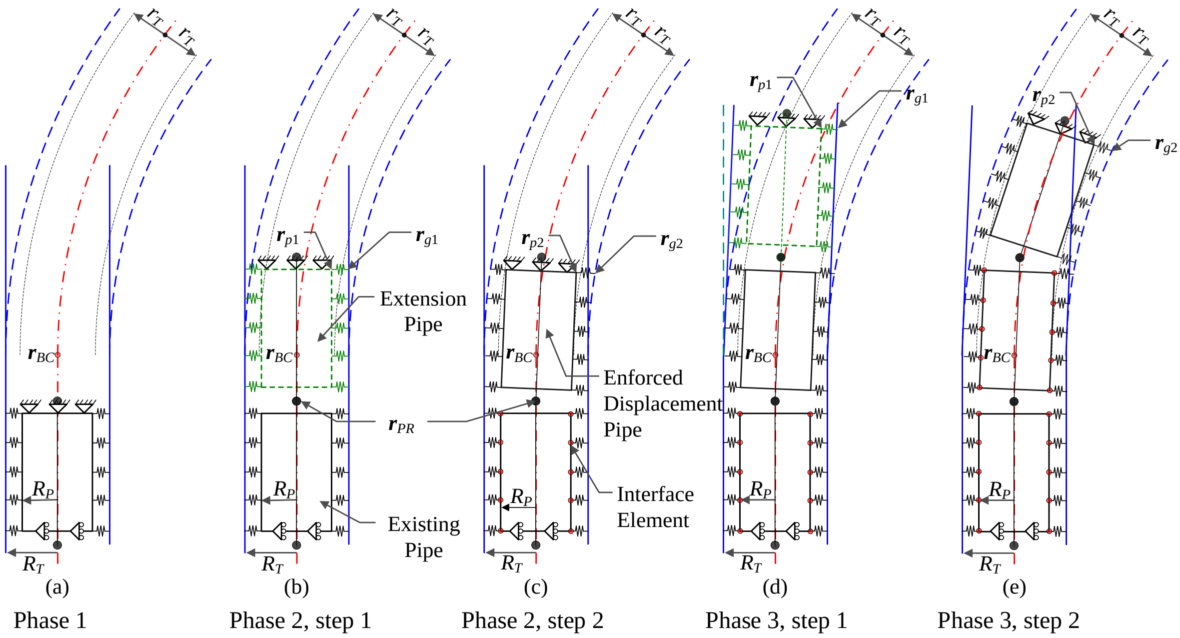

Figure 12 Schematic of phase of analysis procedure (Sugimoto and Asanprakit 2010)

The first phase, illustrated in Figure 12(a), sets the pipes, ground springs, and joint springs along the first straight line, which are defined in Type 1. Boundary conditions are set as fixed at front end of the last pipe, outer end of the ground springs and fixed in radial and circumferential directions at rear end of the first pipe, and free in axial direction. The initial surrounding pressure is applied as pre-stress through the ground springs.

The second phase comprises two steps. The first step involves attachment of new pipe and reset boundary conditions, as shown in Figure 12(b). The new pipe including ground springs and joint springs added to the previous pipe is attached in the same direction of the previous pipe. As new boundary conditions, the fixed boundary condition at the front end of the previous pipe is released; new fixed condition is applied at the outer end of the ground springs and at the front end of the added pipe; and pre-stress representing initial surrounding pressure is applied to the ground springs. Subsequently in the second step, enforced displacement to the outer end of the ground springs in the added pipe and the front end of the added pipe is implemented to achieve the position of Type 2, as shown in Figure 12(c). Simultaneously, the interface elements which represent for friction resistance between the surrounding ground and pipe periphery are installed between the added pipes and added ground springs in the previous phase.

Similar to the second phase, the next phase is executed for the pipe which is placed along the curve alignment (Type 3) or in the transient position from the curved alignment to the next straight alignment (Type 4), illustrated in Figure 12(d and e). When both the last pipe and the next pipe are in the same straight alignment (Type 1), the first phase is applied.

Table 2 Classification of pipe position

Positioning Type	PF	PR
1	Straight	Straight
2	Straight	Curve
3	Curve	Curve
4	Curve	Straight

Last phase, the front end of the last pipe is connected to the machine springs applied with pre-stress to represent the earth pressure at rest acting on the tunnel face, and the pipe end nodes are tied together to reserve the cross-section shape of the pipe. In addition, the interface elements are installed between the added pipes and the added ground springs in the previous phase. Jack force in axial direction is applied at the rear end of the first pipe.

3.4 Simulation

The simulation of the experiments was carried out for the cases of straight and curved alignment, using the finite element software DIANA ver. 9.4 package. Curved shell elements – quadrilateral 4 nodes element were employed to model the concrete pipes and the steel ring. The properties of the concrete pipe and the steel ring are shown in Table 3. Surrounding pressure at the zones involving the rubber sheets was modelled with the translation 2 nodes element. EPS installed at the joint between Pipe II and the steel ring, at the joint between the two concrete pipes, and at the joint between Pipe I and the concrete abutment by translation 2 nodes element. Friction resistance between the pipe peripheries and the concrete shell supports was represented by Mohr-Coulomb friction implemented by interface elements of two nodes, in three-dimensional configuration. The characteristics of interface element which were determined by experiment include friction constant of 0.05 and non cohesion.

Table 3 Properties of concrete pipe and steel ring

Property	Abbreviation	Unit	Value	
			Concrete pipe	Steel ring
Length	L	m	2.43	0.33
Inner diameter	D_{in}	m	0.8	0.8
Thickness	t	m	0.08	0.08
Density	γ	kN/m^3	24	78
Young's modulus	E	kN/m^2	3.8x10^7	2.8x10^8
Poisson's ratio	ν	-	0.17	0.17

The three-dimensional model comprises of 1418 nodes and 1358 elements as illustrated in the Figure 13. The ground springs and the joint springs between Pipe I and the concrete abutment were fixed at the outer ends. Along the bottom of the pipes, horizontal rollers were employed to support the pipes in the vertical direction while allow movement in horizontal direction. Joint springs were applied in three directions for the joint between the steel ring and Pipe II, the joint between the two concrete pipes, and the joint between Pipe I and the concrete abutment. The initial force of 20kN for each jack equivalent to pre-stressed load of 0.694kN was applied for each ground spring. The jack load was implemented at the top and bottom nodes of the steel ring, which represents two thrust jacks of the experiment. Both cases of straight and curved alignments (Case S and Case C), thrust forces of 1000kN were applied. In case of curved alignment (Case C), the enforced displacement at the outer end of the ground spring was applied to mobilize the designed alignment with the crease angle of 3.61 degrees.

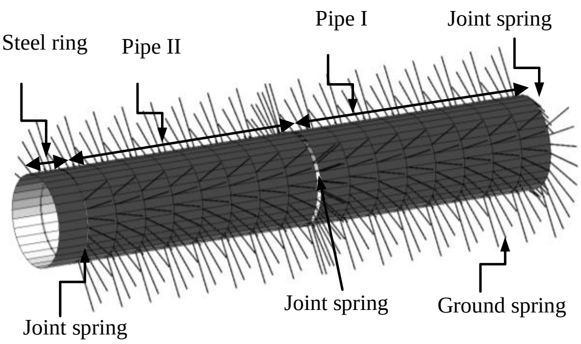

Figure 13 FEM model

4. RESULTS AND DISCUSSION

The measured strain and the calculated strain are shown in the contour maps, in which the horizontal axis represents the pipe length, and the vertical axis is the circumferential direction of the pipe with the origin taken from the invert. In the contour maps, the measured points are shown by circular marks. Due to the limited number of the strain gauge around the opposite side of the pipe joint, it is noted that the contour lines have low accuracy except for around the measured points.

4.1 Pipe response in axial direction

Figure 14 shows the strain in axial direction for the straight alignment (Case S). From this figure, the following were found:

1) For the experimental result, the strain distributes quite symmetric around the vertical plain along the axial direction, in which the maximum compression strain occurs along the top and bottom lines. Compression strain mainly appears from 135 to 225 degrees and from 315 to 45 degrees where the EPS was equipped.
2) For the FEM result, the strain is more symmetric and quite uniform distribution along the zones including the EPS.
3) The tendency of the strain distribution and the magnitude of the strain have a good agreement between the experimental and the FEM results.

Figure 15 shows the strain in axial direction in case of the curved alignment (Case C). From this figure, the following were found:

1) For the experimental result, the compression strain in axial direction maximises at a little lower than 45 degrees and lightly larger than 135 degrees, where are near the edges of the EPS. The strain focuses from 0 to 45 degrees and 135 to 180 degrees where the EPS presents in the concave side of the curve. On the other hand, tensile strain appears at the outer surface of the convex side.
2) The FEM analysis also provided the strain which is well-matched to the experimental result.

Force can be determined from the experiment as follows

$$\varepsilon(x)=\frac{1}{2}(\varepsilon_1+\varepsilon_2)+\frac{\varepsilon_2-\varepsilon_1}{t}x \tag{9}$$

$$N=\int_{-\frac{t}{2}}^{\frac{t}{2}}E\varepsilon(x)dx \tag{10}$$

where ε_1 and ε_2 are strains at the inside and outside of the pipe surface, as shown in Figure 16, t is the thickness of the pipe, and E is Young's modulus of the pipe.

Figures 17 and 18 show the forces in axial direction for the straight and curved alignments, respectively. From these figures, the following were found:

1) The force distribution is very much alike to the distribution of the strains.
2) The force in axial direction mainly presents at the top and bottom for the straight alignment case, and at from 0 to 45 degrees and from 135 to 180 degrees for the case of curved alignment.

These findings can be considered as follows:

1) Thrust force is transferred to the next pipe through EPS at the joint. Therefore stress concentration appears where EPS is placed.
2) Figure 19 shows the distribution of the deformation and the stress of the EPS along the circumferential direction in case of the curved alignment. Here the gap at the joint between two pipes can be calculated based on the crease angle and the movement of the pipe in axial direction during jacking. Then displacement of the EPS is obtained. Stress on the pipes resulted from the deformation of the EPS can be calculated based on the stress-strain relationship of the EPS. From this figure, it can be understood that stress concentration appears at the EPS in the concave side of the curve and consequently horizontal moment is exerted to the pipes by jack force, as shown in Figure 20. These cause the stress distribution in axial direction for the curved alignment.

4.2 Pipe response in circumferential direction

Figure 21 shows the strain in circumferential direction for the straight alignment. From this figure, the following were found:

1) The strain in circumferential direction is much smaller than the strain in axial direction, and the tensile strain is generated in a wide area.
2) For the experimental result, at the inner surface, the strain at the pipe end is compressive at the top and bottom and tensile at the left and right sides, and the strain distribution at the center of the pipe length is reverse. In contrast, at the outer surface, compression appears at the left and right sides and tension appears at the top and bottom. Furthermore, the strain is more concentrated near the joint.
3) For the FEM result, the strain distribution and magnitude at the inner surface and outer surface are similar to the experimental results.

Figure 22 shows the strain in circumferential direction for the curved alignment. It shows that the tendency of the strain distribution is similar to the case of straight alignment.

These findings can be explained as follows:

1) Since the pipe rotation due to the horizontal moment generated by the EPS is restricted by the rigid concrete shell supports, the strain distribution at the pipe ends comes from stress concentration at the edge of the concrete shell support and at the left and right sides as shown in Figure 23, and that at the center of the pipes comes from stress release at the left and right sides which results from the stress concentration at the edge of the concrete shell support. This situation does not appear in practice.
2) The strain distribution around the joint comes from the Poisson's effect as shown in Figure 24.

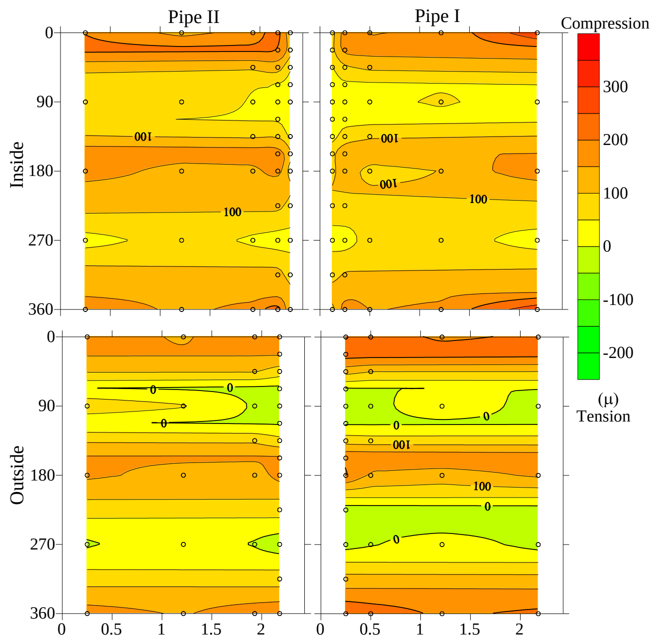

(a) Experiment

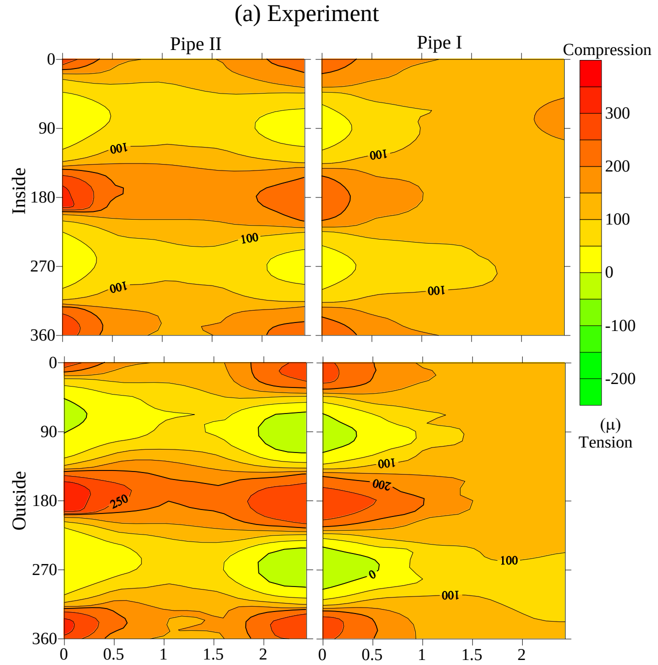

(b) FEM result

Figure 14 Strain in axial direction (Case S)

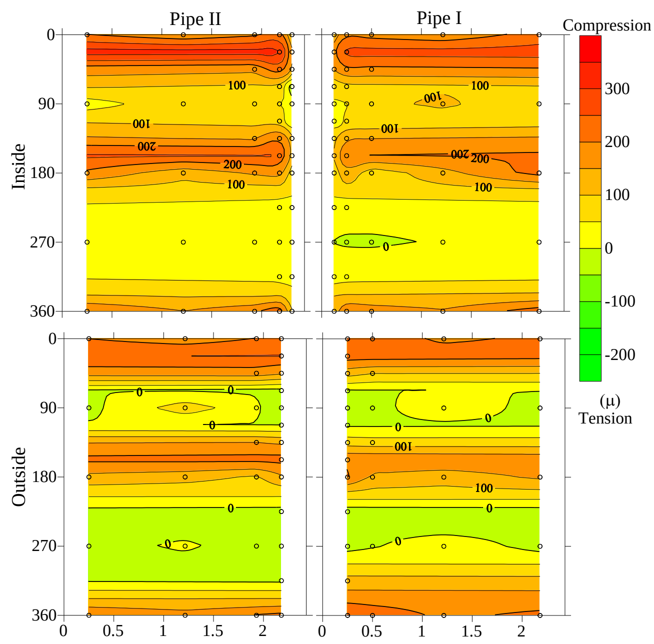

(a) Experimental result

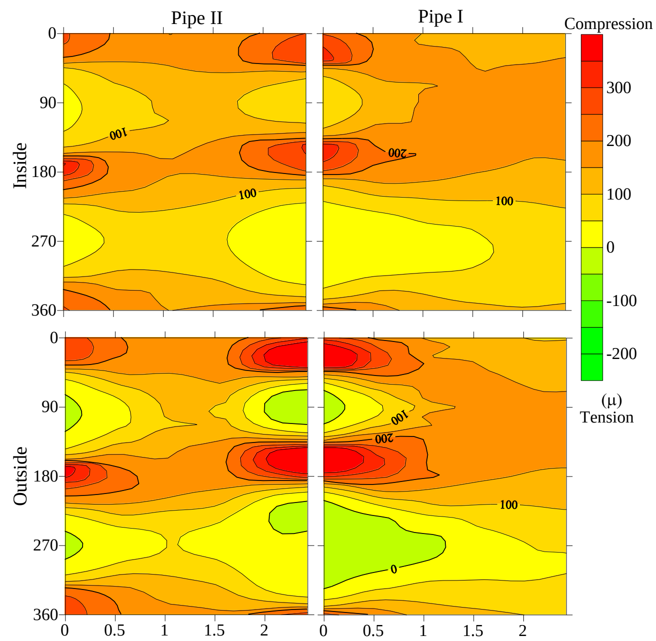

(b) FEM result

Figure 15 Strain in axial direction (Case C)

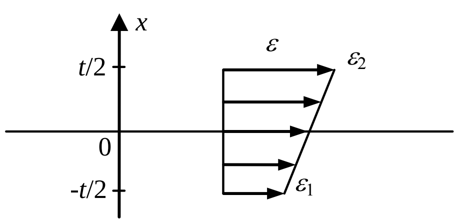

Figure 16 Stress distribution profile

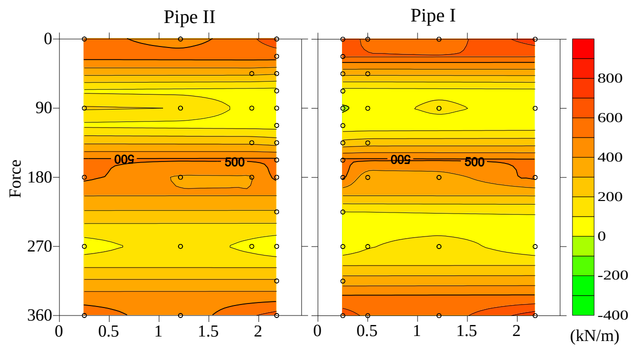

(a) Experimental result

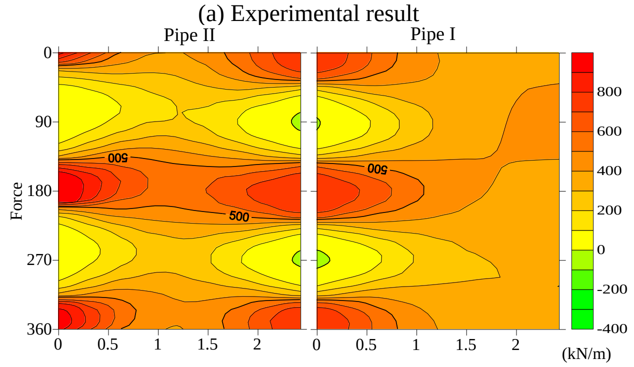

(b) FEM result

Figure 17 Force in axial direction (Case S)

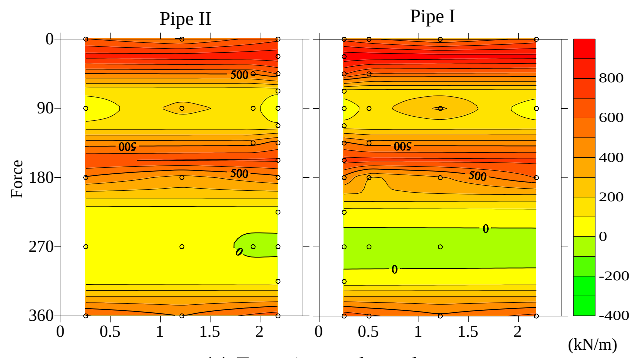

(a) Experimental result

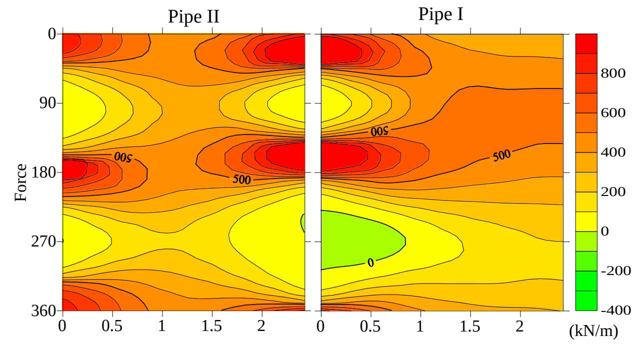

(b) FEM result

Figure 18 Force in axial direction (Case C)

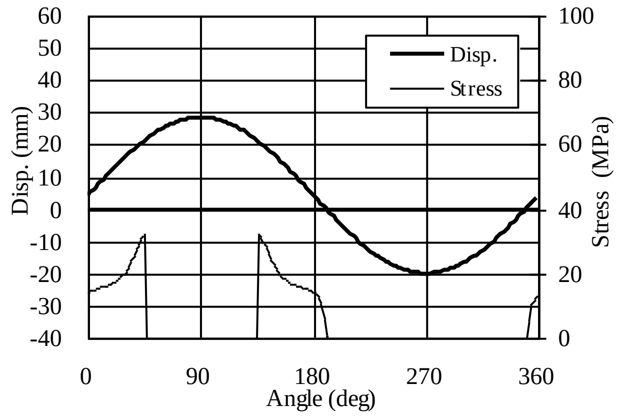

Figure 19 EPS displacement and stress distribution (Case C)

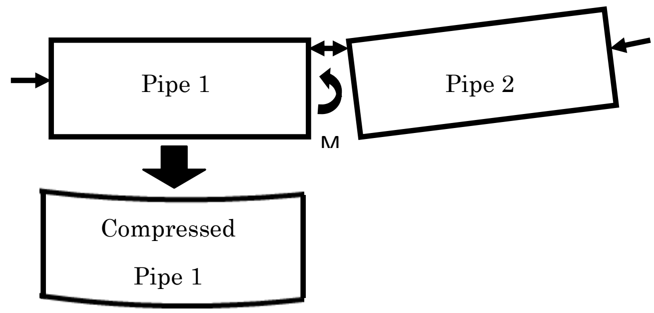

Figure 20 Moment generated due to bending

4.3 Sprincipal strain vector

The principal strain vector was calculated at the positions installed the strain gauges in 0, 45, and 90 degrees. Figure 25 shows the principal strain vector for the straight alignment. From the figure, the following were found:

1) Compressive principal strain appears in axial direction at the top and bottom of the pipes, that is, around the EPS placed and its magnitude decreases as away from the joint. At the outer surface, the direction of the compressive principal strain disperses to the right and left sides of the pipes according to away from the joint. On the other hand, at the inner surface, this tendency is not clear. Furthermore, the compressive principal strain at the outer surface is larger than that at the inner surface.
2) Tensile principal strain appears in circumferential direction, and its magnitude decrease as away form the joint. At the inner surface, tensile principal strain appears at the left and right sides of the pipes. On the contrary, at the outer surface, that appears at the top and bottom of the pipes.

These findings can be considered as follows:

1) The distribution and direction of the compressive principal strain can be explained as the same way as the strain in axial direction, and those of the tensile principal strain can be explained as the same way as the strain in circumferential direction.
2) Since stiffness of the steel is about ten times larger than that of concrete in table 3, steel collar at the outer surface around the joint as shown in Figure 4 transmits larger stress in axial direction at the outer surface, compared with that at the inner surface. Therefore, the compressive principal strain at the outer surface is larger and more dispersed.

Figure 26 shows the principal strain vector for the curved alignment. From this figure, the following were found:

1) The tendency of principal strain is similar to the straight alignment except for the below.
2) Compressive principal strain concentrates on the concave side of the curve and it disperses to the left and right sides of the pipes at not only the outer surface but also the inner surface. It is considered that this comes from the strain concentration at the concave side of the curve.

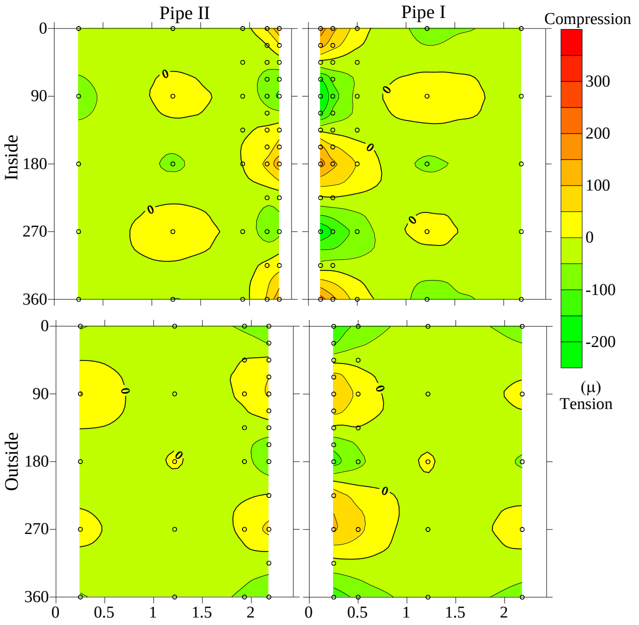

(a) Experimental result

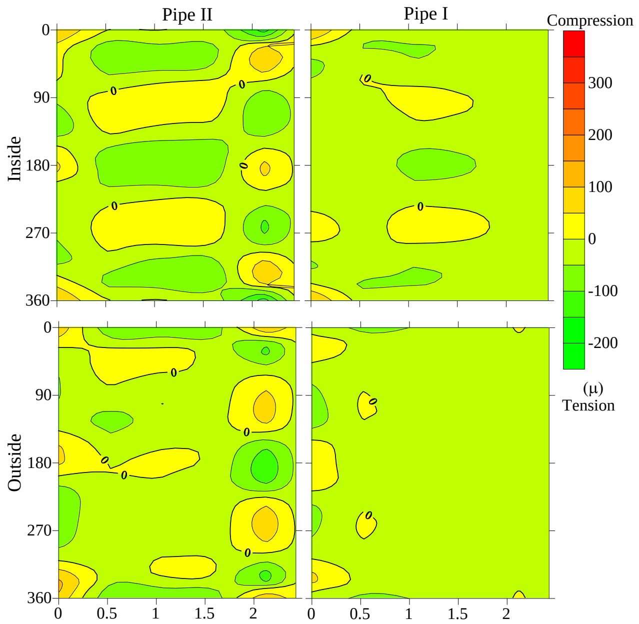

(b) FEM result

Figure 21 Strain in circumferential direction (Case S)

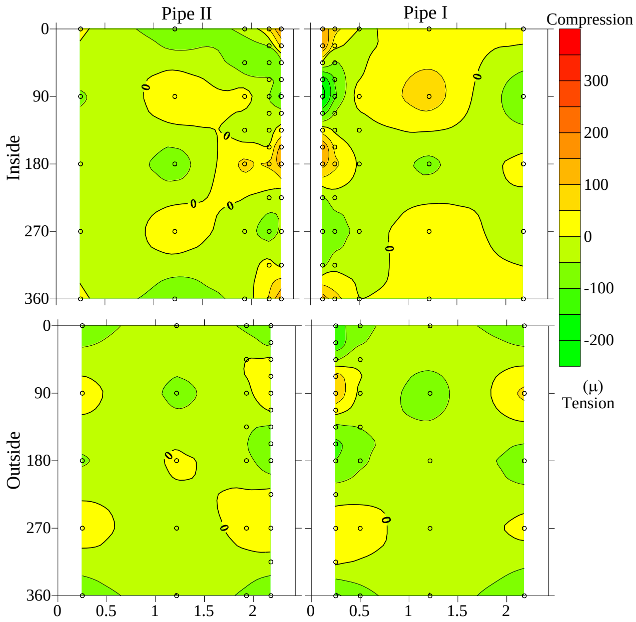

(a) Experimental result

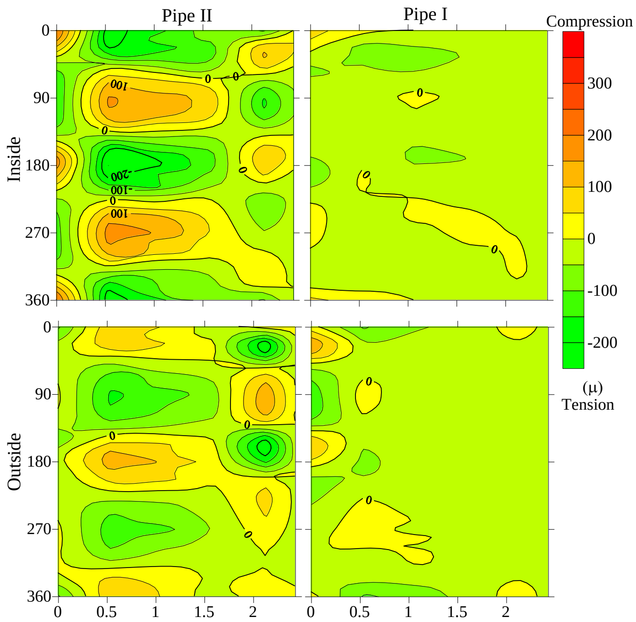

(b) FEM result

Figure 22 Strain in circumferential direction (Case C)

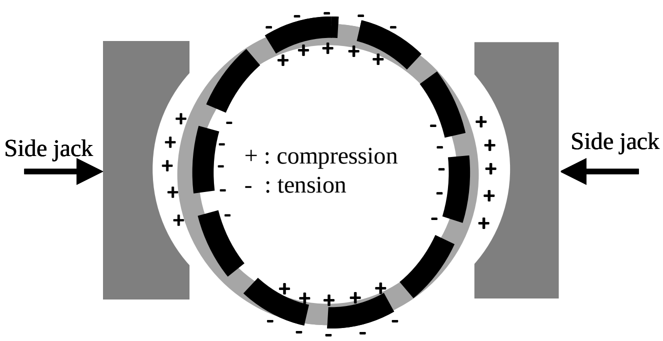

Figure 23 Deformation of pipe due to side jack

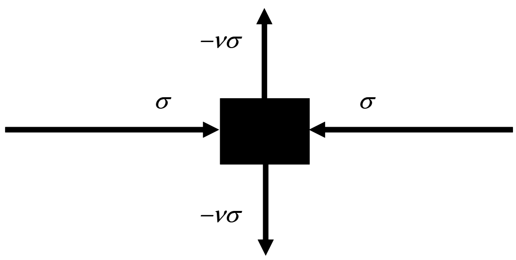

Figure 24 Poisson's effect

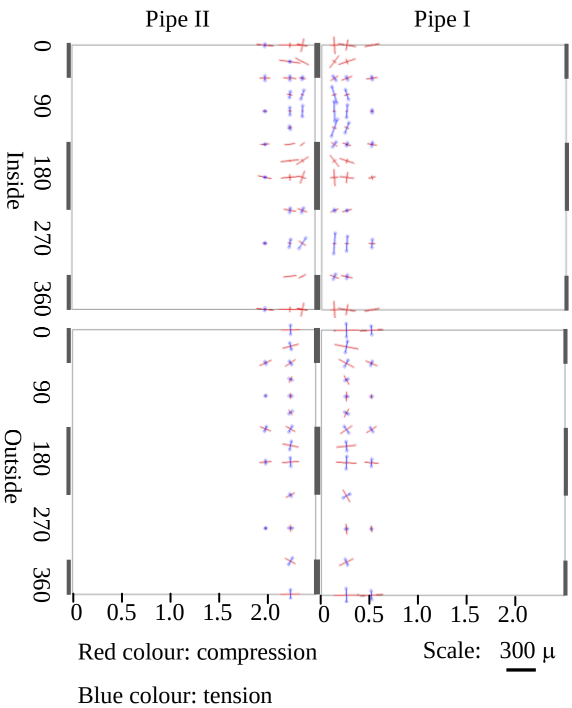

Figure 25 Principal strain vector (Case S)

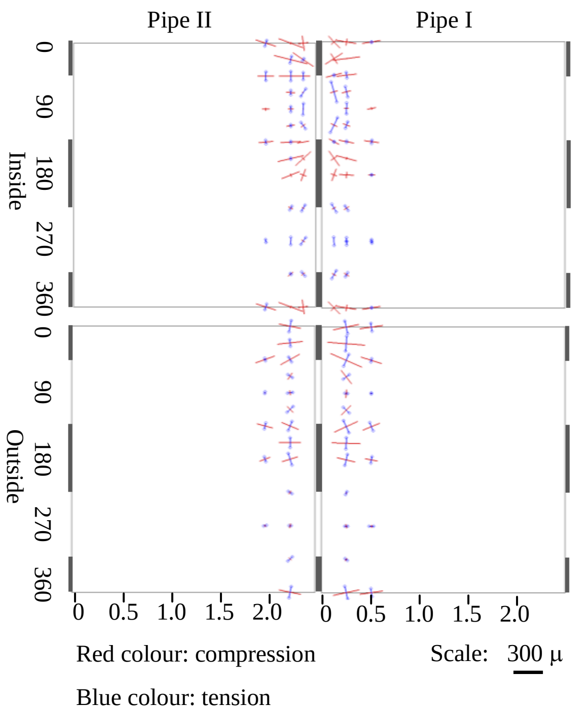

Figure 26 Principal strain vector (Case C)

5. CONCLUSION

To study the joint effect on pipes in pipe jacking method, the full scale tests and the numerical analysis using the stack pipe model were carried out. As a result, the following were concluded.

1) EPS as a cushion material at the joint generates stress concentration and horizontal moment to the pipes in the curved alignment. It causes stress concentration in the axis direction of the pipes where the EPS is placed. Therefore, in pipe design, stress distribution on the pipe within EPS zone, particularly for curved alignment, should be taken into consideration.
2) The stack pipe model can simulate the strain distribution in axial and circumferential direction obtained by the full scale tests reasonably.

As a further research, the stack pipe model should be validated with site data.

6. ACKNOWLEDGMENT

This work was supported by MEXT/JSPS KAKENHI Grant Number 21360205.

7. REFERENCES

Bert, B., and Bernhard, F. (2008) "Simulation of pipe-jacking: Computer model and 1: 1 scale tests", The 26th International Conference and Exhibition for Trenchless Technologies.

Dietmar, B., Robert, S., Tobias, F., and Adrian, U. (2007) "Cojack – A new statics method of computing and controlling pipe jacking", Tunnelling and Underground Space Technology, 22(5-6), pp587-599.

French Society for Trenchless Technology. (2006) Microtunneling and Horizontal Drilling, ISTE Ltd., London, p342.

Pellet-Beaucour, A.-L., and Kastner, R. (2002) "Experimental and analytical study of friction forces during microtunneling operations", Tunnelling and Underground Space Technology, 17(1), pp83-98.

Peter M., Stefan, T., and Daniel H. (2009) "Hydraulic joint for pipe jacking", Journal of Construction Engineering and Management, 135(6), pp439-447.

Le, G.L., Huynh, N.T., Nakamura, K,. and Sugimoto, M. (2012) "Experiment study on influence of joint to pipes in pipe jacking method", Proceedings of World tunnel congress 2012, Bangkok, Thailand, pp741-743.

Norris, P. (1992) The behaviour of jacked concreted pipes during site installation, PhD thesis, University of Oxford.

Sekisui Plastic Co., Ltd. (2004) Thrust transmission material catalog, Tokyo, Japan.

Sramoon, A., and Sugimoto, M. (1999) "Development on ground reaction curve of shield tunneling", Geotechnical aspects of underground construction in soft ground, Balkema, Rotterdam, The Netherlands, pp437-442.

Sugimoto, M., and Sramoon, A. (2002) "Theoretical model of shield behavior during excavation. I: Theory", Journal of Geotechnical and Geoenvironmental Engineering, 128(2), pp138-155.

Sugimoto, M., and Asanprakit, A. (2010) "Stack pipe model for pipe jacking mothed", Journal of Construction Engineering and Management, 136(6), pp683-692.

TNO DIANA BV. (2010) DIANA 9.4. The Netherlands.